Received: 11 January 2024 | Revised: 26 April 2024 | Accepted: 7 May 2024

DOI: 10.1002/rcm.9775

RESEARCH ARTICLE

Rapid Communications in Mass Spectrometry WILEY

Characterization of spironolactone and metabolites derivatized using Girard's reagent P using mass spectrometry and ion mobility spectrometry

Stephanie M. Jones[1] | Kaylie I. Kirkwood-Donelson[2] | Georgia M. Alexander[1] | Lalith Perera[3] | Serena M. Dudek[1] | Alan K. Jarmusch[2]

[1]Neurobiology Laboratory, Division of Intramural Research, National Institute of Environmental Health Sciences, National Institutes of Health, Research Triangle Park, North Carolina, USA

[2]Immunity, Inflammation, and Disease Laboratory, Division of Intramural Research, National Institute of Environmental Health Sciences, National Institutes of Health, Research Triangle Park, North Carolina, USA

[3]Genome Integrity and Structural Biology Laboratory, Division of Intramural Research, National Institute of Environmental Health Sciences, National Institutes of Health, Research Triangle Park, North Carolina, USA

Correspondence
Alan K. Jarmusch, Immunity, Inflammation, and Disease Laboratory, Division of Intramural Research, National Institute of Environmental Health Sciences, National Institutes of Health, Research Triangle Park, NC 27709, USA.
Email: alan.jarmusch@nih.gov

Funding information
National Institute of Environmental Health Sciences, Grant/Award Numbers: Z01 ES043010, Z01 ES100221, ZIC ES103363

Rationale: Spironolactone is a steroidal drug prescribed for a variety of medical conditions and is extensively metabolized quickly after administration. Measurement of spironolactone and its metabolites remains challenging using mass spectrometry (MS) due to in-source fragmentation and relatively poor ionization using electrospray ionization. Therefore, improved methods of measurements are needed, particularly in the case of small sample volumes.

Methods: Girard's reagent P (GP) derivatization of spironolactone was employed to improve response and provide an MS-based solution to the measurement of spironolactone and its metabolites. We performed ultra-high-performance liquid chromatography-electrospray ionization-tandem mass spectrometry (UHPLC-ESI-MS/MS) and ion mobility spectrometry (IMS)–high-resolution mass spectrometry (HRMS) to fully characterize the GP derivatization products. Analytes were studied in positive ionization mode, and MS/MS was performed using nonresonance and resonance excitation collision-induced dissociation.

Results: We observed the successful GP derivatization of spironolactone and its metabolites using authentic chemical standards. A signal enhancement of 1–2 orders of magnitude was observed for GP-derivatized versions of spironolactone and its metabolites. Further, GP derivatization eliminated in-source fragmentation. Finally, we performed GP derivatization and ultra-high-performance liquid chromatography–high-resolution mass spectrometry (UHPLC–HRMS) in a small volume of murine serum (20 µL) from spironolactone-treated and control animals and observed multiple spironolactone metabolites only in the spironolactone-treated group.

Conclusions: GP derivatization was proven to have advantageous mass spectral performance (e.g., limiting in-source fragmentation, enhancing signals, and eliminating isobaric analytes) for spironolactone and its metabolites. This work and the detailed characterization using ultra-high-performance liquid chromatography–high-resolution tandem mass spectrometry (UHPLC–HRMS/MS) and IMS serve as the foundation for future developments in reaction optimization and/or quantitative assay development.

1 | INTRODUCTION

Spironolactone is a synthetic steroid and competitive mineralocorticoid receptor antagonist. The compound was first reported in 1959 when it was initially evaluated for its efficacy as a potassium-sparing diuretic on oral administration.[1] Currently, spironolactone is prescribed for a variety of conditions, including hyperaldosteronism, hypertension, alopecia, acne, and neonatal heart failure.[2–6] Therapeutic outcomes are achieved through the several active metabolites of spironolactone after rapid and extensive metabolism by the liver.[7] Due to its broad indications and extensive biological activity, pharmacokinetic studies are warranted for the compound and its metabolites, as well as their accurate detection in biofluids. Sensitive detection of spironolactone and its metabolites is especially crucial for small sample inputs, as would be the case for minimally invasive samples (e.g., finger-stick or heel-stick samples) or specimens collected from animal models (e.g., repeat tail vein sampling from mice) in translational studies.

Spironolactone and its metabolites are challenging analytes to measure. Early attempts utilized fluorescent and ultraviolet detection systems after chromatographic separation.[8–10] Liquid chromatography (LC) is a method in which chemicals are separated by interactions with a stationary phase immediately prior to mass spectrometry (MS) in which the mass of neutral molecules is measured via gas-phase charged surrogates. Previous reports have noted the challenges specific to spironolactone analysis, including chromatographic separation between spironolactone and metabolites, canrenone, and 7α-thiomethylspironolactone.[11–15] Chromatographic separation is imperative to distinguishing spironolactone and canrenone, as spironolactone undergoes in-source fragmentation during electrospray ionization (ESI) yielding an identical gas-phase ion structure to canrenone, making them indistinguishable using MS as well as tandem mass spectrometry (MS/MS) (viz, *m/z* isolation, collisional activation, and measurement of the product ions resulting from fragmentation).[12] Sufficient chromatographic separation of spironolactone and canrenone has been reported but required unique solvent compositions (methanol–water + 10 mM ammonium acetate, 58%:42%, v/v)[11] or additives such as ammonium fluoride.[12] The work by Takkis et al.[12] demonstrated the ability to measure spironolactone, canrenone, and 7α-thiomethylspironolactone from 50 µL of blood plasma. The success of their analysis was due in part to the ~70-fold increase in signal using ammonium fluoride. The use of additives has pros (e.g., enhanced signal) and cons (e.g., production of hazardous hydrogen fluoride), so alternatives strategies are warranted. One alternative strategy periodically used in the measurement of steroids[16–18] and steroid-like drugs[19] is ion mobility spectrometry (IMS). IMS is a gas-phase technique that separates ions based on their size, shape, and charge by evaluating their mobility through an inert gas under the influence of an electric field.[20] The measured mobility can be used to calculate the ion's collision cross section (CCS), a physiochemical property related to the ion's gas-phase size. The added selectivity of CCS in the analysis of spironolactone and its metabolites could be beneficial in complex matrix, but no literature could be found demonstrating the use of IMS for this analyte. Thus, we performed IMS to establish the necessary empirical values for future method development.

In this study, we sought a strategy via derivatization to improve sensitivity without modifying our chromatography that may also be amenable to a wide variety of analyses (e.g., flow injection, IMS, and ambient ionization techniques).[21] Derivatization is a strategy used to change the physiochemical properties of an analyte, such as increasing the surface activity of an analyte in ESI,[22] creating a permanent charge for neutral or poorly ionizable analytes, or otherwise improving sensitivity and/or selectivity of the MS measurement (e.g., reaction of diol sugars with phenylboronic acid to produce phenylboronate esters).[23] Girard's reagent P (GP) is a positively charged hydrazine that covalently reacts with ketones yielding a derivatized chemical with permanent cationic charge (Scheme 1; Scheme S1). GP derivatization is relatively rapid (i.e., minutes) and involves minimal additional handling operations. Girard's reagents were developed principally for the steroid field, and derivatization of endogenous steroids using Girard's reagents, including GP, prior to MS analysis has been reported.[16–18,24–27] However, this approach has been applied to neither the drug spironolactone nor its metabolites.

In this work, we performed GP derivatization on chemical standards of spironolactone and major metabolites and characterized the derivatization products using ultra-high-performance liquid chromatography–high-resolution tandem mass spectrometry (UHPLC–HRMS/MS) and ion mobility spectrometry–high-resolution mass spectrometry (IMS–HRMS). Our characterization results indicate the benefits of GP derivatization for spironolactone and metabolite analysis, including the elimination of in-source fragmentation of spironolactone and improved response of spironolactone and its

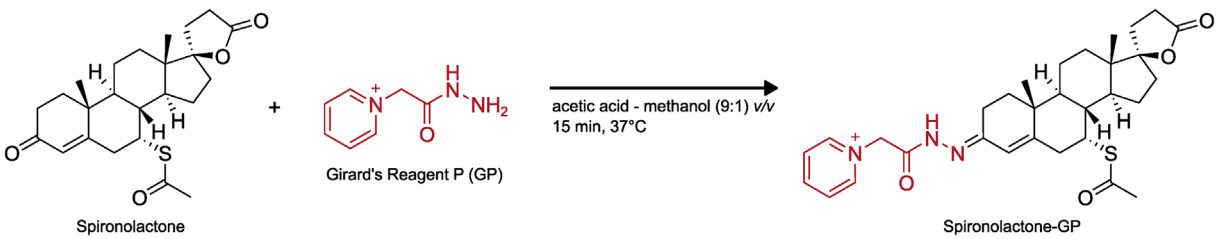

SCHEME 1 Reaction of spironolactone with Girard's reagent P yielding the proposed derivatization product. [Color figure can be viewed at wileyonlinelibrary.com]

metabolites. We characterized the analytes and GP derivatives using MS/MS analysis using nonresonance and resonance excitation methods and report the first IMS measurements (mobility and computed CCS) of the nonderivatized and GP-derivatized analytes. Finally, we demonstrated the ability to perform GP derivatization in a complex biological matrix, that is, murine serum, and detected spironolactone metabolites.

2 | EXPERIMENTAL

2.1 | Derivatization of spironolactone and metabolites

Spironolactone (Cayman Chemical Company, 9000324), canrenone (Cayman Chemical Company, 21307), 7α-thiospironolactone (Toronto Research Chemicals, T375000), 7α-thiomethylspironolactone (Santa Cruz, sc-207187), and 6β-hydroxy-7α-thiomethylspironolactone (Santa Cruz, sc-210569) were purchased from commercial sources and referred to as standards. The standards were reconstituted in methanol–acetic acid (9:1, v/v, 1 mg/mL). Acetic acid was purchased from Supelco (LiChropur). GP was purchased from Toronto Research Chemicals (G388500) and dissolved in1 mg/mL of water (HPLC–MS grade, Fisher Chemical). Two 200-μL aliquots of each standard solution were placed in 2.0-mL autosampler vials (12 × 32 mm-high vial, 12-mm screw cap, and polytetrafluoroethylene/silicone septa, Agilent). To one aliquot of each standard, 20 μL of GP was added; the solution was briefly vortexed and incubated at 37°C for 15 min for derivatization, yielding the GP-derivatized material. Nonderivatized material was made by performing all procedural steps, except the addition of GP (20 μL of HPLC-grade water was added to maintain the same volume), on the second aliquot of each standard. The GP-derivatized and nonderivatized materials were dried using centrifugal evaporation (Genevac EZ-2 Plus, SP Scientific). Immediately prior to analysis, the materials were resuspended in 1 mg/mL of methanol (Optima LC–MS grade, Fisher Chemical). The materials were diluted using methanol and water yielding a stock solution of each analyte at 10 000 ng/mL (*X*) in methanol–water (1:1, v/v). A twofold serial dilution was performed from the stock solution covering the range of *X*–*X*/2048.

2.2 | Murine serum collection

All animal protocols were approved by the National Institute of Environmental Health Sciences Animal Care and Use Committee and were in accordance with the National Institutes of Health guidelines for care and use of animals. To facilitate spironolactone dosing, mice were anesthetized with 2.5% isoflurane and subcutaneously implanted with a slow-release pellet containing 15 mg of the drug (cat. no.: M-161, Innovative Research of America, Sarasota, FL, USA). After 7 days, treated and nondosed control mice ($n = 4$ per group) were killed for serum collection. Mice were killed via rapid decapitation, and trunk blood was funneled into a 1.5-mL microcentrifuge tube. Blood was allowed to coagulate for 15 min at room temperature and then centrifuged for 10 min at 1800 relative centrifugal force (RCF) at 4°C. The serum supernatant was aspirated and stored at −20°C until further analysis.

2.3 | Murine serum sample preparation

On the day of analysis, serum samples were allowed to thaw at 4°C for ∼1 h. Serum was briefly vortexed, and 20 μL was transferred to a 1.5-mL microcentrifuge tube. Eighty microliters of prechilled HPLC-grade methanol was added to precipitate proteins, and the samples were allowed to cool at −20°C for 30 min. The extracts were centrifuged at 14 000 RCF for 10 min at 4°C, and 80 μL of the supernatant was transferred to an autosampler vial. The samples were dried via centrifugal evaporation and resuspended in 200 μL of methanol–acetic acid (9:1, v/v). Twenty microliters of GP was added to each sample and allowed to react for 15 min at 37°C. The samples were dried via centrifugal evaporation and resuspended in 20 μL of methanol–water (1:1, v/v) for analysis.

2.4 | Ultra-high-performance liquid chromatography–high-resolution mass spectrometry

The samples were analyzed using an ultra-high-performance liquid chromatograph (Vanquish Horizon UHPLC, Thermo Scientific) coupled to a high-resolution mass spectrometer (Orbitrap Fusion Tribrid, Thermo Scientific). EASY-Max NG was used as the ionization source, operated in heated-electrospray ionization (H-ESI) configuration. The source parameters in positive ionization mode were as follows: spray voltage, +4000 V; sheath gas, 50 arbitrary units (arb); auxiliary gas, 10 arb; sweep gas, 1 arb; ion transfer tube temperature, 325°C; and vaporizer temperature, 350°C. Prior to measurement, the mass spectrometer was calibrated using FlexMix (Thermo Scientific) following the manufacturer's instructions. EASY-IC (Thermo Scientific) was used during data collection. MS data were acquired at 120 000 resolution from *m/z* 100 to 1000 with a radio frequency (RF) lens of 60% and a maximum injection time of 50 ms. Triplicate injections of the following dilutions were collected for non-GP analytes and GP-derivatized analytes: *X*/2048 (∼4.88 ng/mL), *X*/512 (∼19.5 ng/mL), *X*/128 (∼78.1 ng/mL), *X*/32 (∼313 ng/mL), and *X*/8 (1250 ng/mL).

Chromatographic separation was carried out on a Kinetex F5 analytical column (2.1 mm inner diameter, 100 mm length, 100 Å, 2.6 μm particle size, Phenomenex) with a corresponding guard cartridge. The column was maintained at 30°C during separation. The Vanquish solvent preheater was maintained at 30°C. Gradient elution was performed after an initial period of isocratic elution using water with 0.1% acetic acid (v/v) (A) and acetonitrile with 0.1% acetic acid (v/v) (B). Separation was performed as follows: 0% B from 0 to 2.0 min, 0%–100% B from 2.0 to 10.5 min, 100% B from 10.5 to

12.0 min, 100% to 0% B from 12.0 to 13.0 min, and 0% B from 13.0 to 20.0 min. The flow rate was 500 µL/min. A 10-µL static mixer was used. The post-column flow path consisted of a Viper connection (internal diameter: 0.1 mm, length: 550 mm, Thermo Scientific) from the column to a six-port value and a PEEK tubing from the six-port value to the ionization source.

Data were processed using FreeStyle (ThermoFisher Scientific) and integrated using the default setting for the theoretical monoisotopic mass of each analyte (or GP-derivative) with a mass error of 5 ppm. The peak values were recorded in Excel (Microsoft) and saved as a tab-delimited .txt file. A Jupyter Notebook (R language) was used to compute the mean and standard deviations, and bar plots were constructed using ggplot2.

2.5 | Syringe infusion–HRMS/MS

An Orbitrap Fusion Tribrid (Thermo Scientific) mass spectrometer was used to obtain HRMS and MS/MS measurements from spironolactone, metabolites, and all GP derivatives. Data were collected from materials at 625 ng/mL in methanol–water (1:1, v/v). Data were obtained individually, measured via syringe infusion at 5 µL/min for 1 min. The ionization source conditions were as follows: spray voltage, +2750 V; sheath gas, 2 arbitrary units (arb); auxiliary gas, 2 arb; no sweep gas; ion transfer tube temperature, 275°C; and vaporizer temperature, 0°C. MS data were acquired at a resolution setting of 500 000 from *m/z* 100 to 1000 using an RF lens of 60% and a standard automatic gain control (AGC) target. Data-dependent acquisition was used to obtain MS/MS based on the most intense ions present in the MS scan with a dynamic exclusion of 10 s and a mass tolerance window of 10 ppm. Data were recorded using higher-energy collisional dissociation (HCD) and collision-induced dissociation (CID) at multiple normalized collision energies (NCE). HCD conditions were identical except for NCEs (10, 20, 30, 40, 50, and 60). Quadrupole isolation was used with an isolation window of 1.5 *m/z*, Orbitrap resolution was 30 000; AGC target was standard, one microscan; and data were collected in profile mode. CID conditions were identical except for NCEs (10, 20, 30, and 40). The CID conditions were identical to HCD conditions. The activation time was 10 ms, and the activation *q* was 0.25. Data were processed and exported using FreeStyle and complied with Inkscape.

2.6 | Ion mobility spectrometry–high-resolution mass spectrometry

Ion mobility analyses were performed on a timsTOF Pro (Bruker Daltonics, Bremen, Germany) equipped with an ESI source. Standards were directly injected using a syringe pump at a flow rate of 3 µL/min at concentrations of 1 or 10 µg/mL for GP-derivatized and non-GP analytes, respectively. Triplicate measurements were collected to ensure reproducibility of the mobility values. The positive mode ionization source conditions were as follows: capillary voltage, 4.5 kV; endplate offset, 500 V; drying gas at 220°C, 10 L/min; and nebulizer pressure, 2.2 bar. Mass and mobility calibrations were performed using a mixture of sodium formate clusters and the Agilent ESI low-concentration tune mix (Agilent Technologies, Santa Clara, CA) with standards of known mobilities and CCS values. The TIMS (trapped ion mobility spectrometry) device was operated in ultra (maximum resolution; Figure S1) mode with mobility ranges of 0.1, that is, ±0.05 V s/cm^2 from the analyte's observed $1/K_0$. The transfer funnel RF was set to 300 V_{pp}, and an accumulation time of 100 ms was used. TOF MS data were collected from *m/z* 50 to 1300. Measured mobility values were correlated with $^{TIMS}CCS_{N2}$ values using Bruker Data Analysis software. Additional details on IMS measurements and calculations are presented in Table S1.

2.7 | Energy optimization

Energy optimizations were carried out on the compounds and their metabolites using GP. When available, conformations of the initial compounds were extracted from PubChem database. Metabolite structures as well as the structures of other initial compounds unavailable in the PubChem database were produced using GaussView, version 6.1.[28] GP, all compounds, and their various isomers were energy optimized using Gaussian, version 16.C.02,[29] at the B3LYP/6–311++G(d,p) level.

2.8 | LC–HRMS/MS analysis in murine blood

Murine blood samples were analyzed using the same analytical platform, source conditions, and chromatographic conditions described in Section 2.4. However, data-dependent acquisition was performed on these samples to aid in confirmation of GP derivatives in the complex biological matrix. MS/MS data were acquired at 30 000 resolution using an isolation width of 1.5 *m/z*; stepped-assisted HCD was used with energy steps of 20, 35, and 60 NCE, and a maximum injection time of 54 ms. An intensity filter was applied with an intensity threshold of 2.0×10^4. Dynamic exclusion was used with the following parameters: exclude after $n = 3$ times, if occurs within 15 s, exclusion duration of 6 s, a low mass tolerance of 5-ppm mass error, a high mass tolerance of 5-ppm mass error, and excluding isotopes.

3 | RESULTS AND DISCUSSION

3.1 | Addressing the challenge in spironolactone measurement using MS

Analysis of spironolactone using LC–MS/MS reproduced previously reported observations of deleterious in-source fragmentation to *m/z* 341.2110 and unobservable levels of the protonated species ($[M + H]^+$, *m/z* 417.2094) (Figure 1A). Whereas the protonated

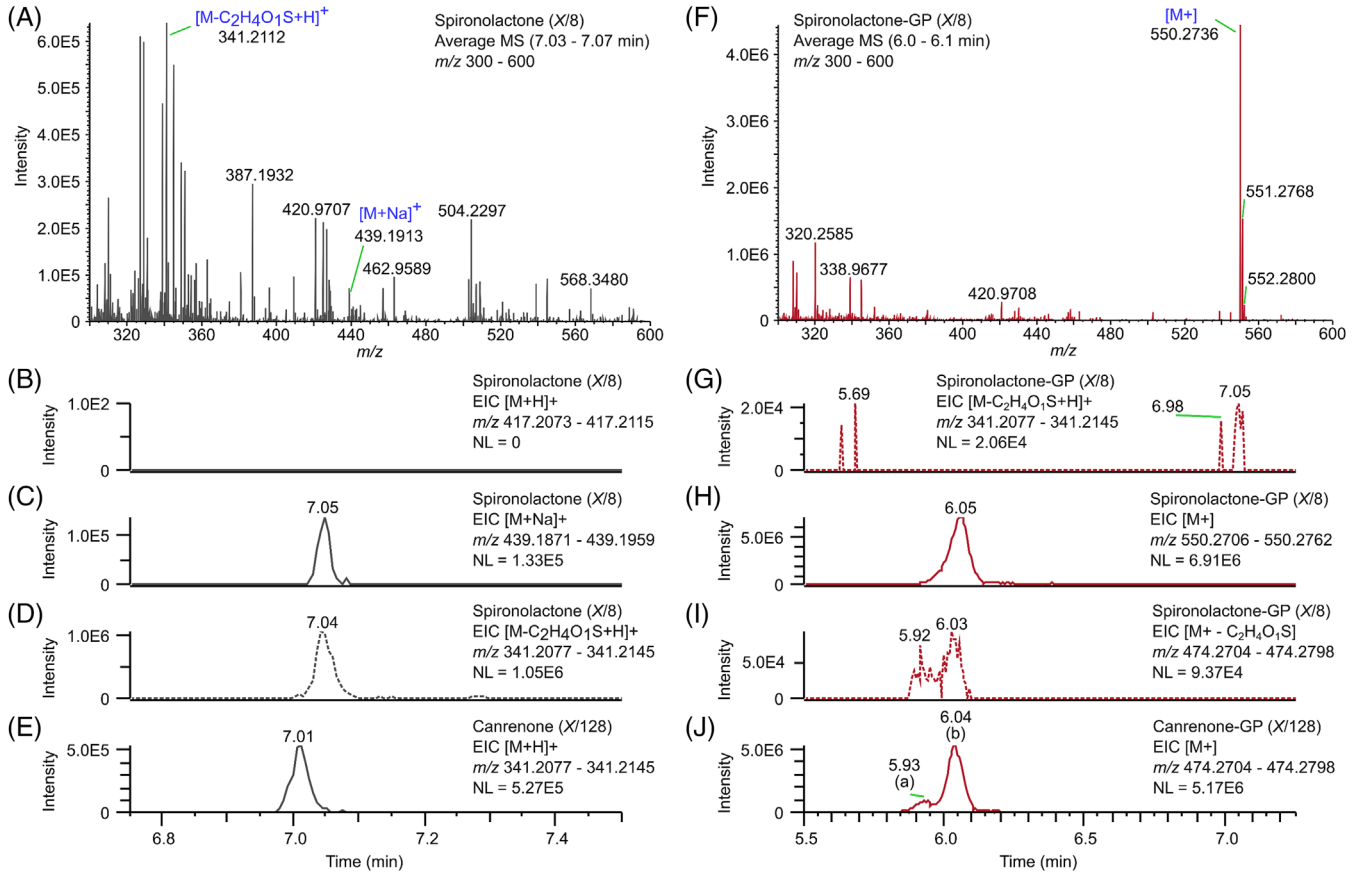

FIGURE 1 Observed spectral differences between spironolactone and spironolactone-GP (Girard's reagent P). (A) Average spectrum from 7.03 to 7.07 min exhibiting *m/z* 300–600 annotated with the observed species associated with spironolactone. Mass range chromatograms for spironolactone (B) protonated species, (C) sodiated species, and (D) in-source fragment (dotted line). (E) Mass range chromatogram for the protonated species of canrenone. (F) Average spectrum from 6.0 to 6.1 min exhibiting *m/z* 300–600 with spironolactone-GP annotated. (G) Mass range chromatogram for the in-source fragment (dotted line) of spironolactone. (H) Mass range chromatogram for the molecular ion of spironolactone-GP and (I) in-source fragment (dotted line) of spironolactone-GP. (J) Mass range chromatogram for canrenone-GP.
Notes: the maximum base peak values are noted in each panel (normalization level [NL]); dotted lines indicate in-source fragments; and canrenone and canrenone-GP were plotted using more dilute samples for visualization. [Color figure can be viewed at wileyonlinelibrary.com]

species was not observed (Figure 1A,B), the sodiated spironolactone species was observed in positive mode (Figure 1C). The predominant signal observed from the analysis of a spironolactone standard was the in-source fragment, denoted by a dashed trace in Figure 1D. The in-source fragment is isobaric and presumed to be structurally identical to that of canrenone. For this work we did not optimize the chromatographic conditions to separate spironolactone from its metabolites. Despite the lack of chromatographic optimization, the protonated species of canrenone (Figure 1E) and the previously mentioned in-source fragment observed from spironolactone (Figure 1D) were visually resolved. In summary, our observations match those previously reported and recapitulate the need for chromatographic separation given spironolactone's propensity for in-source fragmentation to an isobaric structure similar, if not identical, to canrenone.

In contrast, the reaction of spironolactone with GP, that is, spironolactone-GP, yielded a clear mass spectral signal. The spectrum shown in Figure 1F contains a predominant M^+ ion of *m/z* 550.2736, matching that of spironolactone-GP (0.36 ppm). There was no evidence of unreacted spironolactone (protonated or sodiated species) in the spironolactone-GP *X*/8 sample. The predominant in-source fragment of spironolactone was also not observed (Figure 1G), further supporting reaction efficiency. Spironolactone-GP was readily observed with a chromatographic peak at 6.05 min (Figure 1H). GP derivatization stabilized the precursor ion. In-source fragmentation was not observed in the mass spectrum (Figure 1F) and a minor peak was observed in the extracted ion chromatogram (Figure 1I). The rationale for this observation is unknown; however, quaternary amines are relatively stable, and the addition of GP to the structure of spironolactone may serve to stabilize the thioester group that is lost during ionization of nonderivatized spironolactone. The limited in-source fragmentation from spironolactone-GP eliminates the isobaric interference with canrenone-GP and thus reduces the dependency of chromatographic separation. Indeed, analysis of canrenone-GP (Figure 1J) resulted in the observation of *m/z* 474.2750 at 6.04 min (peak b).

A lesser-abundant isobaric peak (a) with identical MS/MS product ion spectra (Figure S2) was observed in the case of canrenone. This observation suggests a side product imparting either constitutional isomerism or stereoisomerism. The identical MS/MS observation, although dominated by GP-related observations (e.g., neutral loss of the pyridine heterocycle), does not support or refute a constitutional isomer. The possibility of a stereoisomer cannot be excluded, and separation is theoretically possible in our experimental apparatus (e.g., pentafluorophenyl propyl stationary phase chemistry).

To explore the impact of GP derivatization on the analysis of common spironolactone metabolites, we additionally investigated 7α-thiospironolactone, 7α-thiomethylspironolactone, and 6β-hydroxy-7α-thiomethylspironolactone. The predicted reaction product structures (Scheme S1) and details are presented in Table 1. As in the case of spironolactone-GP, all GP-derivatized analytes tested yielded dominant precursor ion signals resulting from the molecular ion species. Further, all GP reaction products exhibited lesser retention times, which conforms to the expectation that more polar substances elute earlier.

3.2 | Signal enhancement observed in GP derivatives

One of our aims was to determine the ability of GP derivatization to increase signal. In Figure 2, equal amounts of each chemical, nonderivatized or GP derivatized, are compared to demonstrate the increased signal. In all cases, the extracted ion chromatograms of GP reaction products exhibited greater signal intensity (i.e., peak height) as well as integrated peak area. Further, we arbitrarily selected the concentration of 312.5 ng/mL (*X*/32) and assessed the mean and relative standard deviation in peak area between technical triplicates. Notably, the GP-related increase was not uniform in spironolactone or its metabolites. For example, canrenone (∼15×) was observed to benefit the least from GP derivatization, whereas 6β-hydroxy-7α-thiomethylspironolactone (∼846×) benefited the greatest. The observed increase in signal matches expectations of the introduction of a quaternary amine in the pyridine ring of GP. This removes the acid–base chemistry of ionization via ESI that is necessary in the formation of protonated species. However, the introduction of the charged species alters the surface activity of the molecule in electrospray droplets. The opposed effects may explain, in part, the differential increase in signal.

3.3 | Characterization of GP reaction products

Given the novel nature of applying GP derivatization to spironolactone and its metabolites, we characterized the GP reaction products using HRMS and MS/MS, and in doing so affirmed the predicted reaction products and provided reference data. Syringe infusion–HRMS/MS measurements acquired from nonreacted and GP-derivatized standards made on an Orbitrap mass analyzer at a

TABLE 1 Empirical measurements of spironolactone and spironolactone metabolites analyzed using UHPLC–HRMS/MS and IMS.

Chemical	Molecular formula	Species	Theoretical *m/z*	Measured *m/z*[a]	Mass error (ppm)	^{34}S isotope[a]	Retention time (min)[b]	$1/K_0$[c]	CCS (Å^2)[c]
Spironolactone	$C_{24}H_{32}O_4S$	$[M+H]^+$	417.2094	n.d.	n.d.	n.d.	n.d.	n.d.	n.d.
Spironolactone	$C_{24}H_{32}O_4S$	$[M+Na]^+$	439.1915	439.1917	0.46	Yes	7.05	1.004	207.4
Spironolactone-GP	$C_{31}H_{40}N_3O_4S$	M^+	550.2734	550.2736	0.36	Yes	6.06	1.209	248.2
Canrenone	$C_{22}H_{28}O_3$	$[M+H]^+$	341.2111	341.2110	−0.29	No	7.01	0.887	184.8
Canrenone-GP	$C_{29}H_{36}N_3O_3$	M^+	474.2751	474.2750	−0.21	No	6.04	1.121	231.0
7α-Thiospironolactone	$C_{22}H_{30}O_3S$	$[M+H]^+$	375.1988	375.1989[b]	0.27[b]	Yes[b]	6.97	0.931	193.3
7α-Thiospironolactone	$C_{22}H_{30}O_3S$	$[M+Na]^+$	397.1808	397.1807	−0.25	Yes	6.97	n.d.	n.d.
7α-Thiospironolactone-GP	$C_{29}H_{38}N_3O_3S$	M^+	508.2628	508.2636	1.57	Yes	6.00	1.156	237.8
7α-Thiomethylspironolactone	$C_{23}H_{32}O_3S$	$[M+H]^+$	389.2145	389.2148	0.77	Yes	7.02	0.946	196.1
7α-Thiomethylspironolactone-GP	$C_{30}H_{40}N_3O_3S$	M^+	522.2785	522.2787	0.38	Yes	6.03	1.174	241.3
6β-Hydroxy-7α-thiomethylspironolactone	$C_{23}H_{32}O_4S$	$[M+H]^+$	405.2094	405.2097	0.74	Yes	6.33	0.966	200.0
6β-Hydroxy-7α-thiomethylspironolactone-GP	$C_{30}H_{40}N_3O_4S$	M^+	538.2734	538.2733	−0.19	Yes	5.40	1.190	244.4

Abbreviations: CCS, collision cross section; GP, Girard's reagent P; HRMS, high-resolution mass spectrometry; IMS, ion mobility spectrometry; UHPLC, ultra-high-performance liquid chromatography.
[a]Syringe infusion–HRMS/MS.
[b]UHPLC–HRMS.
[c]IMS–HRMS.

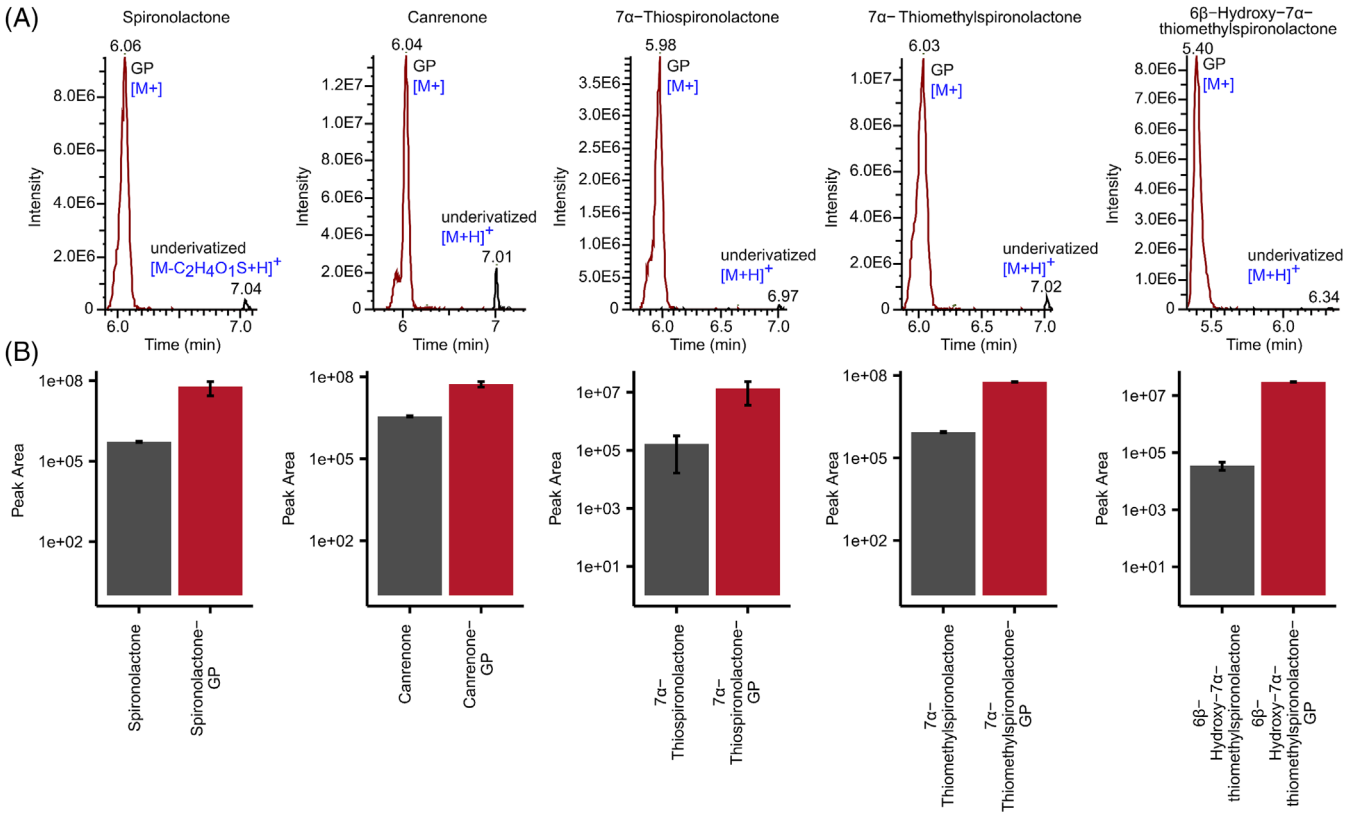

FIGURE 2 Comparison between nonderivatized and GP (Girard's reagent P)–derivatized analytes of spironolactone and its metabolites. (A) Extracted ion chromatograms for nonderivatized chemical (black trace) and GP derivative (red trace). (B) Bar plots showing the mean and relative standard deviation in peak area (technical triplicates). Data shown for 7α-thiospironolactone include $n = 2$ technical replicates. [Color figure can be viewed at wileyonlinelibrary.com]

resolution setting of 500 000 yielded measured accurate masses of less than two part per million (ppm) (Table 1; Figures S3–S12). For example, the [M+] species of spironolactone-GP was measured at *m/z* 550.2736, which deviates by 0.36 ppm from the theoretical *m/z* of 550.2734. Further, sulfur-containing analytes were confirmed to have the correct isotopic distribution for ^{34}S (~4.2%). In summary, the HRMS data supported all molecular formulae for the nonderivatized analytes and the GP-derivatized analytes.

We established the MS/MS product ion spectra obtained from spironolactone, its metabolites, and all GP-derivatized analytes. Data were acquired with multiple collision energies using nonresonance excitation HCD and resonance excitation CID. The MS/MS results for GP-derivatized analytes agree with those reported in literature for other GP derivatives.[16,25–27] We observed the characteristic neutral loss of *m/z* 79.0422 corresponding to the pyridine heterocycle, C_5H_5N, present in GP. For example, fragmentation of canrenone-GP (Figure S3) yielded a product ion at *m/z* 395.2321. Interestingly, fragmentation of spironolactone-GP using HCD and CID (minimum 30 NCE) yielded the same product ion at *m/z* 395.2321 (Figure S4), indicating that on activation the pyridine heterocycle is lost as well as the thioester group of spironolactone-GP. We determined the approximate range of NCE for HCD and CID of the analytes as defined by 90% reduction in the precursor *m/z* signal. In general, optimal NCEs for both HCD and CID dissociations were higher for GP analytes compared to nonreacted analytes, supportive of an increase in stability of quaternary amines. Optimal HCD energies for canrenone (Figure S5), 7α-thiomethylspironolactone (Figure S6), and 6β-hydroxy-7α-thiomethylspironolactone (Figure S7) were approximately 40–50, 20–30, and 20–30 NCE, respectively. For CID, optimal energies ranged from 20 to 30, 20 to 30, and 10 to 20 NCE for these same analytes, respectively. The optimal HCD energies for the derivatized precursor *m/z* values for spironolactone-GP (Figure S4), canrenone-GP (Figure S3), 7α-thiospironolactone-GP (Figure S8), 7α-thiomethylspironolactone-GP (Figure S9), and 6β-hydroxy-7α-thiomethylspironolactone-GP (Figure S10) ranged from 40 to 60 NCE. The optimal CID energies were 20–30, 10–20, 20–30, 30–40, and 30, respectively. We were not able to generate spectra for all chemicals, for example, the protonated and sodiated species of spironolactone, due to low signal and poor MS/MS, respectively.

We performed TIMS–HRMS analysis to further characterize the gas-phase size and shape of the analytes as well as GP reaction products. There were no reports of CCS values for the analytes tested (nonderivatized or GP derivatized) except canrenone. Our $^{TIMS}CCS_{N2}$ value for canrenone was less than 1% different from the reported value,[19] supporting the quality of our reported ion mobility data. We were able to observe all analytes and their corresponding GP products

(Table 1). As in the LC–HRMS experiments, we did not detect the protonated ion of spironolactone and thus could determine neither its mobility ($1/K_0$) nor CCS. However, sodiated spironolactone was detected, and we report its IMS values here. Notably, we observed a similar increase in signal for GP derivatives compared to nonderivatized analytes in our IMS–MS measurements.

Mobility and CCS values increased for GP-derivatized counterparts of spironolactone's metabolites, consistent with the increased molecular size of reaction products, as shown in Figure 3 and Figures S13–S16. Linear relationships between *m/z* and CCS were observed for nonderivatized ($R^2 = 0.9992$) and GP-derivatized ($R^2 = 0.9945$) analytes (Figure S17). For canrenone, 7α-thiospironolactone, and 7α-thiomethylspironolactone, we observed two distinct mobilities for each nonderivatized analyte, where each primary peak had a CCS value approximately 1%–2% larger than the lower-abundance peak (Table 1; Figure 3; Figures S12–S16). This result may be due to the gas-phase conformational flexibility of some steroids, which has been shown to produce multiple mobilities in previous high-resolution IMS analyses.[30,31] Alternatively, we cannot rule out impurities or stereoisomers in the standards used (purity listed as 95% or greater). For canrenone-GP, 7α-thiospironolactone-GP, and 7α-thiomethylspironolactone-GP, a primary peak with an unresolved shoulder was observed for each, suggesting GP derivatization may have stabilized the gas-phase structures relative to their nonderivatized counterparts given its planar nature.[16] For spironolactone-GP, it appears the mobility is treading toward two peaks (Figure S12). It is unclear whether this pattern similarly suggests the presence of multiple gas-phase conformers or distinct reaction products occurring on different carbonyls of the compound, as nonderivatized spironolactone could not be measured for comparison.

As an initial investigation into the empirical mobility data, we performed modeling on spironolactone and metabolites without and with GP derivatization. Illustrative structures are shown in Figure S18. The resulting energy-optimized structures for GP-derivatized structures support the possibility of multiple structural conformers, typically with rotation in the nitrogen–nitrogen bond of the hydrazone formed with GP derivatization. The difference in energy between the conformers is within the typical range of internal energy deposition during ESI (a few eV) with the following ranges: spironolactone-GP, 0.38 eV; canrenone-GP, 0.40 eV; 7α-thiospironolactone-GP, 0.39 eV; 7α-thiomethylspironolactone-GP, 0.38 eV; and 6β-hydroxy-7α-thiomethylspironolactone-GP, 0.42 eV. The presence of multiple conformers may be reflected in the ion mobility data as the broadness of the measured inverse mobility peaks as well as the trend toward some peaks having what appear to be unresolved shoulders. Further modeling of the gas-phase structures would be needed to fully contextualize the TIMS results.

3.4 | Demonstration of GP derivatization in biological matrix—serum

To demonstrate the biological applicability of the proposed GP derivatization approach, MS measurements of spironolactone and metabolites were made in serum of mice implanted with a slow-release pellet containing spironolactone. Samples from treated animals were processed in parallel with serum from control animals to facilitate comparison. Spironolactone-GP was detected neither in the treated mice nor in the control mice (Figure 4A). Despite the improved spironolactone detection afforded by GP, the

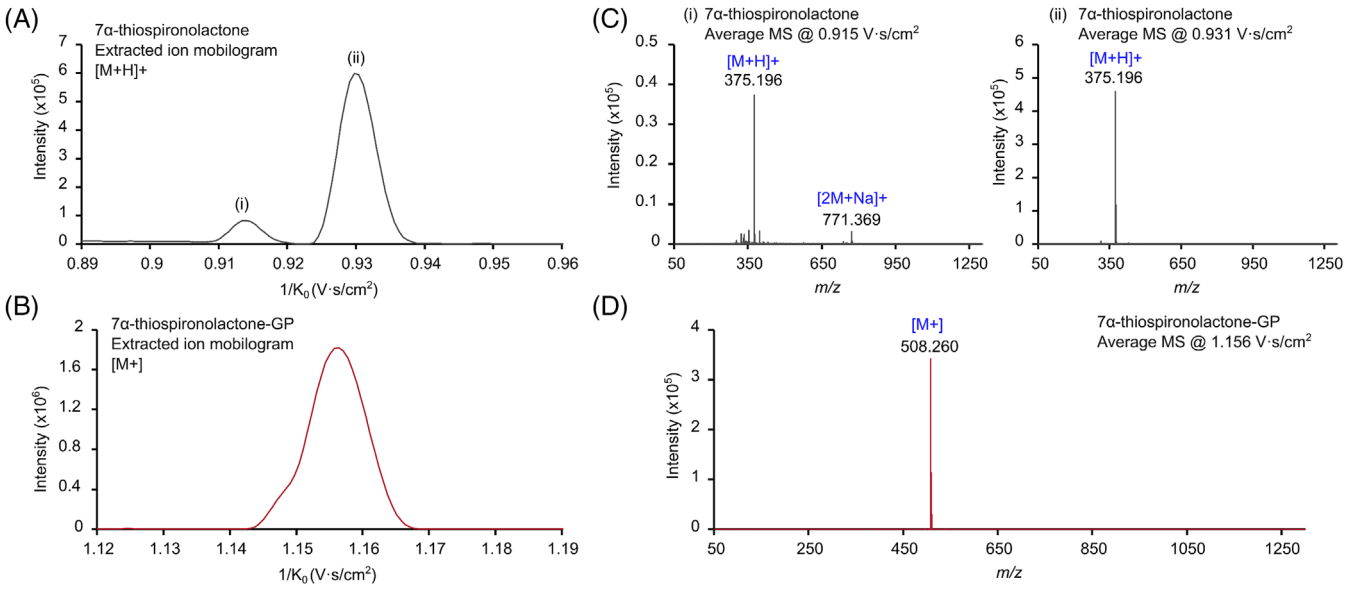

FIGURE 3 Illustrative example of TIMS (trapped ion mobility spectrometry) measurements of 7α-thiospironolactone and 7α-thiospironolactone-GP (Girard's reagent P). Extracted ion mobilograms of (A) 7α-thiospironolactone, $[M + H]^+$, *m/z* 375.196; and (B) 7α-thiospironolactone-GP, [M+], *m/z* 508.260. Average mass spectrum collected for (C) 7α-thiospironolactone at (i) 0.915 and (ii) 0.931 V s/cm^2 and (D) 7α-thiospironolactone-GP at 1.156 V s/cm^2. [Color figure can be viewed at wileyonlinelibrary.com]

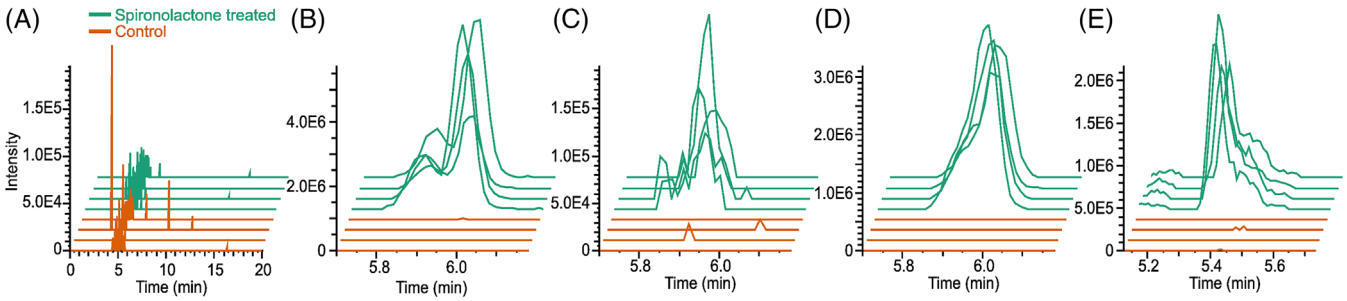

FIGURE 4 Demonstration of spironolactone and spironolactone metabolite GP (Girard's reagent P) derivatization and observation in biological matrix. Extracted ion chromatograms of (A) spironolactone-GP, (B) canrenone-GP, (C) 7α-thiospironolactone-GP, (D) 7α-thiomethylspironolactone-GP, and (E) 6β-hydroxy-7α-thiomethylspironolactone-GP from GP-derivatized serum in control (orange trace) and spironolactone-treated mice (teal trace). [Color figure can be viewed at wileyonlinelibrary.com]

spironolactone concentration in the serum could be present below the observable level. Biologically, the lack of observable spironolactone-GP could reflect the rapid metabolism of spironolactone in vivo ($\lambda = 1.4$ h).[12,32] The latter, biological rationale, is supported by the detection of canrenone-GP, 7α-thiospironolactone-GP, 7α-thiomethylspironolactone-GP, and 6β-hydroxy-7α-thiomethylspironolactone-GP in the treated mice, none of which were detected in controls, Figure 4B–E. The half-lives of canrenone, 7α-thiomethylspironolactone, and 6β-hydroxy-7α-thiomethylspironolactone are also much longer than that of spironolactone, $\lambda = 16.5$, 13.8, and 15.0 h, respectively.[32] Therefore, we postulate that our observation of spironolactone's metabolites but not spironolactone itself is primarily due to in vivo metabolism.

3.5 | Limitations

We did not optimize the reaction conditions for GP derivatization in standard solution nor in biological samples as these parameters (reaction time, pH, temperature, etc.) are likely matrix and application specific. However, we have laid the foundation for characterization and demonstration of utility in a biological matrix. Additionally, we did not assess these initial findings for the viability as a quantitative approach as it was beyond the scope of the initial work in the characterization of the reaction products. Regarding the biological application, we did not intend to comment on the biological outcome or the improvement in the detection efficiency between nonderivatized and GP analytes as that comparison is better performed on optimization of the reaction conditions, preanalytical steps (e.g., extraction method), and analytical steps (e.g., instrumentation, acquisition mode, column chemistry).

4 | CONCLUSIONS

Spironolactone and its metabolites are important analytes to measure given their broad indications and extensive biological activity. Importantly, most in vivo work is performed in animal models from which samples are often limited, particularly in the case of blood from repeated tail vein sampling in rodents. Similarly, minimally invasive methods of sampling human biofluids produce small samples. We sought to explore the capability of GP to derivatize spironolactone and its metabolites to address previously observed behaviors that were detrimental to analytical measurement. These disadvantageous effects include extensive (if not complete) in-source fragmentation that necessitates chromatographic separation and relatively poor ionization efficiency of spironolactone and downstream metabolites. We performed GP derivatization on standards and observed more ideal mass spectral behavior in the elimination of in-source fragmentation, a singular dominant molecular ion species, and improved signal response. We measured the GP reaction products (and spironolactone analytes) using HRMS and confirmed the molecular formulae, matching within 2-ppm mass error, and ^{34}S isotopic pattern. Tandem MS data supported a GP reaction product, and we characterized the MS/MS product ion scans using CID and HCD over multiple NCEs. Further, we utilized IMS to measure the mobility and computed CCSs of the GP reaction products (and spironolactone metabolites). These are the first-reported IMS values for the analytes and GP products, except for canrenone, which matched literature value within 1%.[19] Finally, to demonstrate the ability of the GP derivatization approach to be compatible with analysis in a biological, in vivo sample, we exhibit the detection of spironolactone metabolites specifically in the serum of dosed mice. In sum, these findings demonstrate the benefits of GP derivatization for improved detection of spironolactone and its metabolites from chemical standards, with practical utility demonstrated in an illustrative biological matrix. Future work will be needed to optimize the reaction conditions, which are likely to be matrix specific, to develop a quantitative method, and to evaluate utility for ambient ionization techniques.

AUTHOR CONTRIBUTIONS

Stephanie M. Jones: Writing—review and editing; investigation; methodology; formal analysis; writing—original draft; data curation; visualization; conceptualization. **Kaylie I. Kirkwood-Donelson:** Investigation; methodology; formal analysis; visualization; writing—

original draft; writing—review and editing; conceptualization. **Georgia M. Alexander:** Writing—original draft; writing—review and editing; project administration; supervision. **Lalith Perera:** Methodology; formal analysis; visualization; writing—review and editing; funding acquisition; resources; investigation. **Serena M. Dudek:** Supervision; resources; writing—review and editing; writing—original draft; funding acquisition; project administration. **Alan K. Jarmusch:** Funding acquisition; writing—original draft; writing—review and editing; project administration; resources; supervision; formal analysis; conceptualization; investigation.

ACKNOWLEDGMENT

This research was supported by the Intramural Research Program of the NIH, National Institute of Environmental Health Sciences (ZIC ES103363, Z01 ES043010, and Z01 ES100221).

DATA AVAILABILITY STATEMENT

The data that support the findings of this study are openly available in MassIVE at https://doi.org/10.25345/C55H7C515, reference number MSV000094621.

ORCID

Serena M. Dudek https://orcid.org/0000-0003-4094-8368

REFERENCES

1. Cella JA, Tweit RC. Steroidal aldosterone blockers. II. *J Org Chem*. 1959;24(8):1109-1110. doi:10.1021/jo01090a019
2. Conn JW, Hinerman DL. Spironolactone-induced inhibition of aldosterone biosynthesis in primary aldosteronism: morphological and functional studies. *Metabolism*. 1977;26(12):1293-1307. doi:10.1016/0026-0495(77)90026-9
3. Wolf RL. Treatment of hypertension with spironolactone. *JAMA*. 1966;198(11):1143. doi:10.1001/jama.1966.03110240051022
4. Famenini S, Slaught C, Duan L, Goh C. Demographics of women with female pattern hair loss and the effectiveness of spironolactone therapy. *J Am Acad Dermatol*. 2015;73(4):705-706. doi:10.1016/j.jaad.2015.06.063
5. Charny JW, Choi JK, James WD. Spironolactone for the treatment of acne in women, a retrospective study of 110 patients. *Int J Women's Dermatol*. 2017;3(2):111-115. doi:10.1016/j.ijwd.2016.12.002
6. Hobbins SM, Fowler RS, Rowe RD, Korey AG. Spironolactone therapy in infants with congestive heart failure secondary to congenital heart disease. *Arch Dis Child*. 1981;56(12):934-938. doi:10.1136/adc.56.12.934
7. Los LE, Pitzenberger SM, Ramjit HG, Coddington AB, Colby HD. Hepatic metabolism of spironolactone. Production of 3-hydroxy-thiomethyl metabolites. *Drug Metab Dispos*. 1994;22(6):903-908.
8. Gochman N, Gantt CL. A fluorimetric method for the determination of a major spironolactone (aldactone) metabolite in human plasma. *J Pharmacol Exp Ther*. 1962;135(3):312-316.
9. Sadee W, Dagcioglu M, Riegelman S. Fluorometric microassay for spironolactone and its metabolites in biological fluids. *J Pharm Sci*. 1972;61(7):1126-1129. doi:10.1002/jps.2600610719
10. Jankowski A, Shorek-Jankowksi A, Lamparczyk H. Simultaneous determination of spironolactone and its metabolites in human plasma. *J Pharm Biomed Anal*. 1996;14(8–10):1359-1365. doi:10.1016/S0731-7085(96)01767-0
11. Vlase L, Imre S, Muntean D, Achim M, Muntean D. Determination of spironolactone and canrenone in human plasma by high-performance liquid chromatography with mass spectrometry detection. *Croatica Chemica Acta*. 2011;84(3):361-366. doi:10.5562/cca1761
12. Takkis K, Aro R, Kõrgvee L-T, et al. Signal enhancement in the HPLC-ESI-MS/MS analysis of spironolactone and its metabolites using HFIP and NH4F as eluent additives. *Anal Bioanal Chem*. 2017;409(12):3145-3151. doi:10.1007/s00216-017-0255-4
13. Ferreira-Nunes R, Almeida EATD, Cunha-Filho M, Gratieri T, Gelfuso GM. Liquid chromatography-mass spectrometry for simultaneous determination of spironolactone and canrenone in plasma samples. *Braz J Pharm Sci*. 2023;59:59. doi:10.1590/s2175-97902023e21626
14. Sora DI, Udrescu S, Albu F, David V, Medvedovici A. Analytical issues in HPLC/MS/MS simultaneous assay of furosemide, spironolactone and canrenone in human plasma samples. *J Pharm Biomed Anal*. 2010;52(5):734-740. doi:10.1016/j.jpba.2010.03.004
15. Dong H, Xu F, Zhang Z, Tian Y, Chen Y. Simultaneous determination of spironolactone and its active metabolite canrenone in human plasma by HPLC-APCI-MS. *J Mass Spectrom*. 2006;41(4):477-486. doi:10.1002/jms.1006
16. Velosa DC, Dunham AJ, Rivera ME, Neal SP, Chouinar CD. Improved ion mobility separation and structural characterization of steroids using derivatization methods. *J am Soc Mass Spectrom*. 2022;33(9):1761-1771. doi:10.1021/jasms.2c00164
17. Rāciņš O, Nagy G. Implementation of charged microdroplet-based derivatization of bile acids on a cyclic ion mobility spectrometry-mass spectrometry platform. *Anal Methods*. 2023;15(42):5577-5581. doi:10.1039/d3ay01447a
18. Neal SP, Hodges WN, Velosa DC, Aderorho R, Lucas SW, Chouinard CD. Improved analysis of derivatized steroid hormone isomers using ion mobility-mass spectrometry (IM-MS). *Anal Bioanal Chem*. 2023;415(27):6757-6769. doi:10.1007/s00216-023-04953-8
19. Hines KM, Ross DH, Davidson KL, Bush MF, Xu L. Large-scale structural characterization of drug and drug-like compounds by high-throughput ion mobility-mass spectrometry. *Anal Chem*. 2017;89(17):9023-9030. doi:10.1021/acs.analchem.7b01709
20. Viehland LA, Mason EA. Gaseous ion mobility in electric fields of arbitrary strength. *Ann Phys Rehabil Med*. 1975;91(2):499-533. doi:10.1016/0003-4916(75)90233-X
21. Feider CL, Krieger A, DeHoog RJ, Eberlin LS. Ambient ionization mass spectrometry: Recent developments and applications. *Anal Chem*. 2019;91(7):4266-4290. doi:10.1021/acs.analchem.9b00807
22. Cech NB, Enke CG. Practical implications of some recent studies in electrospray ionization fundamentals. *Mass Spectrom Rev*. 2001;20(6):362-387. doi:10.1002/mas.10008
23. Heiss DR, Badu-Tawiah AK. Liquid chromatography–tandem mass spectrometry with online, in-source droplet-based phenylboronic acid derivatization for sensitive analysis of saccharides. *Anal Chem*. 2022;94(40):14071-14078. doi:10.1021/acs.analchem.2c03736
24. Wheeler OH. The Girard reagents. *J Chem Educ*. 1968;45(6):435. doi:10.1021/ed045p435
25. Frey AJ, Wang Q, Busch C, et al. Validation of highly sensitive simultaneous targeted and untargeted analysis of keto-steroids by Girard P derivatization and stable isotope dilution-liquid chromatography-high resolution mass spectrometry. *Steroids*. 2016;116:60-66. doi:10.1016/j.steroids.2016.10.003
26. Rangiah K, Shah SJ, Vachani A, Ciccimaro E, Blair IA. Liquid chromatography/mass spectrometry of pre-ionized Girard P derivatives for quantifying estrone and its metabolites in serum from postmenopausal women. *Rapid Commun Mass Spectrom*. 2011;25(9):1297-1307. doi:10.1002/rcm.4982
27. Yuan Y, Xu Y, Lu J. Detection of 20 endogenous anabolic steroid esters with Girard's reagent P derivatization in dried blood spots using UPLC-Q-Orbitrap-MS. *J Chromatogr B*. 2022;1213(1213):123535. doi:10.1016/j.jchromb.2022.123535
28. GaussView; Semichem Inc. 2016.

29. Gaussian 16; Gaussian, Inc. 2016.
30. Feuerstein ML, Hernández-Mesa M, Kiehne A, et al. Comparability of steroid collision cross sections using three different IM-HRMS technologies: an interplatform study. *J am Soc Mass Spectrom*. 2022; 33(10):1951-1959. doi:10.1021/jasms.2c00196
31. Chouinard CD, Cruzeiro VWD, Beekman CR, Roitberg AE, Yost RA. Investigating sifferences in gas-phase conformations of 25-hydroxyvitamin D3 sodiated epimers using ion mobility-mass spectrometry and theoretical modeling. *J am Soc Mass Spectrom*. 2017;28(8):1497-1505. doi:10.1007/s13361-017-1673-4
32. Gardiner P, Schrode K, Quinlan D, et al. Spironolactone metabolism: Steady-state serum levels of the sulfur-containing metabolites. *J Clin Pharmacol*. 1989;29(4):342-347. doi:10.1002/j.1552-4604.1989.tb03339.x

SUPPORTING INFORMATION

Additional supporting information can be found online in the Supporting Information section at the end of this article.

How to cite this article: Jones SM, Kirkwood-Donelson KI, Alexander GM, Perera L, Dudek SM, Jarmusch AK. Characterization of spironolactone and metabolites derivatized using Girard's reagent P using mass spectrometry and ion mobility spectrometry. *Rapid Commun Mass Spectrom*. 2024;38(15):e9775. doi:10.1002/rcm.9775